Applied Geochemistry 38 (2013) 92–102

Contents lists available at ScienceDirect

Applied Geochemistry

journal homepage: www.elsevier.com/locate/apgeochem

The role of climate in the accumulation of lithium-rich brine in the Central Andes

L.V. Godfrey [a,b,*], L.-H. Chan [c,3], R.N. Alonso [d], T.K. Lowenstein [e], W.F. McDonough [f], J. Houston [g], J. Li [e,1], A. Bobst [e,2], T.E. Jordan [a]

[a] Department of Earth and Atmospheric Sciences, Cornell University, Snee Hall, Ithaca, NY 14853-1504, USA
[b] Institute of Marine and Coastal Sciences, Rutgers University, 71 Dudley Road, New Brunswick, NJ 08901, USA
[c] Department of Geology and Geophysics, Louisiana State University, Baton Rouge, LA 70803-4101, USA
[d] Universidad Nacional de Salta, CONICET, Buenos Aires 177, 4400 Salta, Argentina
[e] Department of Geological Sciences and Environmental Studies, State University of New York at Binghamton, Binghamton, NY 13902, USA
[f] Department of Geology, University of Maryland, College Park, MA 20742, USA
[g] Stuart Lodge, 273 Wells Road, Malvern WR14 4HH, UK

ARTICLE INFO

Article history:
Received 5 March 2013
Accepted 2 September 2013
Available online 6 September 2013
Editorial handling by M. Kersten

ABSTRACT

Lithium-rich brine within the sub-surface of the Salar del Hombre Muerto (SHM) salt pan in the Andes of northwestern Argentina has a chemical and isotopic composition which is consistent with Li derived from several sources: the modern halite saturated lagoon, Li-rich salts and brines formed recently, and dissolution of halite which precipitated from ancient saline lakes. SHM lies in the closed basin that includes part of the massive Cerro Galán caldera which is drained by the Río los Patos, which is responsible for 90% of surface runoff into the salar. The low Li isotope composition, +3.4‰, of this river is consistent with significant contributions of geothermal spring water. As water drains through the volcaniclastic deposits which cover a large proportion of the basin, Li removal, as indicated by decreasing Li/Na, occurs but without significant isotope fractionation. This indicates a mechanism of surface sorption onto smectite or ferrihydrite rather than Li incorporation into octahedral structural sites of clays. These observations suggest that conditions in this high altitude desert have limited the dilution of hydrothermal spring water as well as the formation of clay minerals, which jointly have allowed the Li resource to accumulate rapidly. Changes in climate on a multi-millennial time scale, specifically in the hydrologic budget, have resulted in solute accumulation rates that have been variable through time, and decoupled Li and Na fluxes. Inflow to the salar under modern conditions has high Li/Na (7.9×10^{-3} by wt) with δ^7Li indistinguishable from basement rocks (−0.3‰ to +6.4‰), while under pluvial climate conditions the Li/Na of the saline lake was 40 times lower than the modern lagoon ($0.1–0.3 \times 10^{-3}$ compared to $10.6–13.4 \times 10^{-3}$) with slightly higher δ^7Li, +6.9‰ to +12.3‰, reflecting the uptake of ^{6}Li into secondary minerals which formed under a wetter climate.

1. Introduction

Concerns associated with fossil fuels have promoted alternative energy strategies, many of which require energy to be stored. The development of high energy density Li-batteries, and in particular their application in hybrid transport technologies has increased the demand for Li many-fold, and the search for new resources. Some of the richest brine sources of Li come from the closed drainage basins of the Central Andes (Evans, 2008). Ide and Kunasz (1989) proposed that Li is derived from one or more of the following processes; (1) low temperature weathering of ash-flow tuffs; (2) geothermal waters associated with active volcanism; (3) Li-rich clays that pre-date volcanic arc activity in this area in which the Li concentration is high due to a local or regional Li anomaly of uncertain origin; and (4) saline water that formed outside the topographic limits of the drainage basin in which it is extracted and that entered the basin through faults. Although Ide and Kunasz were specifically addressing the accumulation of Li in the Salar de Atacama in Chile, which occupies a basin on the western flank of the Andes, the mechanisms which accumulate Li in many of the other salars in the arid Central Andes are expected to be similar (Houston et al., 2011).

An additional factor we consider is climate. Studies in the Central Andes have shown that hydrological conditions have varied

* Corresponding author at: Department of Earth and Planetary Sciences, Rutgers University, 610 Taylor Road, Piscataway, NJ 08854, USA. Tel.: +1 7324453507.
E-mail address: godfrey@marine.rutgers.edu (L.V. Godfrey).
[1] Address: Sempra Energy Trading, 700 Fairfield Ave, Stamford, CT 06902, USA.
[2] Address: Montana Bureau of Mines and Geology, 1300 West Park, Butte, MT 59701, USA.
[3] Deceased.

0883-2927/$ - see front matter © 2013 Published by Elsevier Ltd.
http://dx.doi.org/10.1016/j.apgeochem.2013.09.002

considerably over millennial time scales. Ages of elevated shorelines and lake deposits in currently dry salt pans have been found to coincide with the last glacial maximum in the Puna of Argentina as well as southern Bolivia and Northern Chile (Godfrey et al., 2003; Lowenstein et al., 1996, 2003; Bobst et al., 2001; Fritz et al., 2004; Placzek et al., 2006). An increase in the hydrologic cycle may serve to accelerate weathering in hyper-arid climates, or dilute fluids emanating from hot springs (Gibert et al., 2009), both of which can influence the formation and geochemical composition of brine. This study thus provides the opportunity to study the Li isotope geochemistry and budget of water draining a volcanically active region where climate has altered the hydrologic budget and influenced weathering.

This study focuses on the Hombre Muerto drainage basin and salt pan (salar), located in northwest Argentina within the broader domain of the Puna plateau. The drainage basin of Hombre Muerto is a closed system, so all the products of weathering accumulate in the salar. Changes in climate and hydrologic budget of the region during the late Pleistocene may have altered the relative contributions of Li from different sources and areas of the drainage network, altering the mean weathering flux of the basin. We present chemical and isotopic data for fluids, rocks and chemical sediments from the Salar del Hombre Muerto basin. We use these data to determine the conditions, present and past, under which brine in the Salar del Hombre Muerto has developed with very high concentrations of Li.

2. The geological setting of Salar del Hombre Muerto and its Li reserve

At 4000 m altitude, Salar del Hombre Muerto (SHM) occupies one of many closed drainage basins located on the eastern side of the Puna plateau in northwestern Argentina (Fig. 1a). The salar is renowned for its mineral reserves: Boron is mined at Tincalayu on its northern margin and from the clastic apron formed by the Río los Patos entering the salt pan; and Li is currently extracted from the subsurface brine by FMC at its Fenix plant while a second site, Sal da Vida, is under development by Galaxy Resources.

The 600 km^2 Hombre Muerto salar lies in the northern end of a 4000 km^2 drainage basin (Fig. 1b). The Hombre Muerto drainage basin is filled by young volcanic features overlying Paleozoic crystalline rocks, Paleozoic marine sediments, and Cenozoic continental sediments. Cenozoic volcanic activity in the region began in the early Oligocene with the formation of andesitic stratovolcano Ratones (Linares and González, 1990). Magmatism at Cerro Galán began during the Miocene, and between 2.2 and 2.0 Myr ago erupted 1000 km^3 of ignimbrites (Sparks et al., 1985; Kay et al., 2010a), collectively referred to as the Cerro Galán ignimbrite. Recent shallow seismic swarms of uncertain origin, as well as young scoria cones on the western edge of Cerro Galán indicate continued activity (Risse et al., 2008; Heit et al., 2010).

Numerous faults cross Hombre Muerto basin and the salar (Fig. 1c) creating deep clastic filled relict basins (Jordan et al., 1999; Rosko and Jaacks, 2012). One particular NNW–SSE strike-slip fault identified from surface features and gravity data runs along the western side of Isla Catal and then cuts SW across the salar to Vega Hombre Muerto. The thickness of halite increases by many hundreds of meters to the west of the fault into the halite nucleus of the salar (Jordan et al., 1999). The halite nucleus accounts for almost half the area of SHM and has a rough relief due to the buckling of halite polygons formed under prolonged aridity. Increased hydrologic activity in the past is evidenced by halite preserved from long-lived saline lakes which covered this area 86.0 ± 9.3 Ka ago and 63.8 ± 6.8 Ka ago, as well as from smaller or shorter-lived lakes which occurred within the last 22 Ka (Lowenstein et al., 1996; Godfrey et al., 2003). Laminated carbonate precipitated at a now inactive spring mound around 40 Ka ago (M. Fleisher, pers. comm.) also documents an increased water budget.

The largest source of surface water to the salar is the Rió los Patos which drains almost 80% of the total area of the drainage basin and flows roughly north–south about 150 km from Cerro Galán. Measured flow rates of the Río los Patos typically vary between 0.8 and 2.0 m^3/s. The average flow in 1992, when the precipitation total for the year was 15 mm below a 10-year average of 77.4 mm, was 1.6 m^3/s and represented 90% of surface runoff to the salar (Hombre Muerto EIS, Water Management Consultants, 1992; Rosko and Jaacks, 2012). Most of the remaining10% of surface run-off is accounted for by the Río Trapiche. There are two branches of the Río los Patos which meet close to water sampling location 1. The shorter branch drains Vega Aguas Caliente in the caldera of Cerro Galán through a gap in the northern part of the caldera rim, while the longer branch drains most of the eastern flanks of the caldera and a narrow strip of Paleozoic basement on the western flank of the Eastern Cordillera of the Andes. After these branches join, the river flows approximately 50 km to enter the eastern side of SHM where it then turns to the southwest (Fig 1c). At the southern end of Isla Catal the river forms a lagoon except during dry years when there is insufficient flow and it infiltrates soft sediments. In the eastern area brackish water overlies dense brine while in the western halite nucleus brine is close to the surface and brackish water is confined to narrow mudflats at the edge of the salar.

The Li resource of SHM is contained in the brine which occupies the pore space in most of the sedimentary units in-filling the salar. The Li resource in the eastern and northern sub-basins is estimated to be about 10^9 kg (Rosko and Jaacks, 2012). In the western sub-basin, the effective porosity of halite is 9 ± 3% (1 standard deviation, Hombre Muerto EIS, Water Managament Consultants, 1992), and if similar to the halite-dominated sub-basins, may not change significantly with depth (Lithium One, NI 40-101, 2012). Using an average porosity of 9% and reported mean Li concentration of 650 mg/L (Hombre Muerto EIS, Water Managament Consultants, 1992), some 2.5×10^9 kg of Li are present in the upper 140 m, the average depth of other sub-basins of the salar. Combining these estimates suggest that about 3×10^9 kg of Li, if not more, may exist in SHM brine.

3. Sampling and methodology

3.1. Sample collection

Water from springs and streams were collected between 1996 and 2008 (Fig 1c). Geothermal fluid locations are indicated in Fig. 1b. The description of most of these geothermal systems can be found in Giggenbach (1978), Schmitt et al. (2002), Kasemann et al. (2004) and Cortecci et al. (2005). Water samples were filtered through 0.4 μm polypropylene syringe filters and duplicate samples were stored in polyethylene bottles, acidified for cation and Li and Sr isotope analyses, or unacidified for anion analyses. Acid neutralizing capacity was measured in the field by titration with 0.1 N HCl.

Samples of laminated carbonate and primary lake halite were used to determine the chemistry of lake and inflow waters in the past. Two samples of halite formed in a lake 86.0 ± 9.3 Ka (#351) and 63.8 ± 6.8 Ka (#321) were collected from core #2005 which was used in previous paleohydrology studies of the basin (Lowenstein et al., 1996; Godfrey et al., 2003). Halite crystals were cleaved under a microscope with a razor blade to exclude portions that contained detrital material, other evaporite minerals such as gypsum, or halite cement which could contaminate the sample with modern subsurface fluids. Samples of carbonate were taken from

Fig. 1. (a) Location of Salar del Hombre Muerto; (b) the location of geothermal fluid samples in relation to the volcanic arc, crystalline basement and salars; (c) geologic map of the area surrounding Salar del Hombre Muerto showing the sampling locations (refer to Table 1). Symbols in (c): circles, freshwater sampling locations; squares, brine sampling locations.

the laminated carbonate which forms a spring mound last active about 40 Ka ago located 500 m to the west of the southern end of Isla Catal.

Basement rocks and pegmatites were collected near Mina los Patos. Samples representative of mafic volcanic rocks in the system come from two lavas from Isla Catal. Two samples of the Cerro Galán ignimbrite were collected, a welded and finely crystalline sample from the eastern margin of SHM and a coarsely crystalline one from Vega Hombre Muerto which shows evidence of weathering by bronzing of biotite. Rock powders were digested in closed Teflon vials using ultrapure HF, HNO_3 and HCl acids. Lithium was leached at room temperature from the 2.1 Ma Cerro Galán ignimbrite and ash (LAS-W and LAS-S) from the 1993 eruption of Lascar which lies immediately east of the Salar de Atacama using distilled water for 51 days, following the protocol of Risacher and Alonso (2001).

3.2. Analytical methods

Cation (Na, K, Ca, Mg, and Sr) concentrations were measured with an ARL direct current plasma atomic emission spectrometer (DCP-AES) at Binghamton University or a Varian inductively coupled plasma optical emission spectrometer (ICP-OES) at Rutgers University (geothermal spring waters). Repeated analyses of Hombre Muerto water samples and gravimetric standard solutions gave error estimates of less than ±10% relative standard deviation. Anion (Cl, SO_4, Br) concentrations were measured using a Dionex ion chromatograph at Cornell University. Silicon concentrations were measured by standard additions using a Varian ICP–OES at Rutgers University.

Lithium isotope analyses were either performed at Louisiana State University (LSU) or at the University of Maryland (UMD) as indicated in the data tables. Lithium analyzed by thermal ionization mass spectrometry (TIMS) at LSU was also purified at LSU using the method described in You and Chan (1996). Samples analyzed at UMD for Li isotope compositions were separated at Rutgers University, using 1 N NHO_3 in 80% (v/v) methanol and AG50W-X8 cation resin for rock samples (Tomascak et al., 1999), or 0.25 N HCl and AG50W-X12 cation resin for the water samples. Every sample was checked to insure quantitative Li recovery and separation from Na before it was analyzed for δ^7Li (Jeffcoate et al., 2004). Lithium isotope analyses using the Nu Plasma multi collector inductively coupled plasma mass spectrometer (MC-ICPMS) at the UMD used the standard-bracketing method. Isotope

data are reported as δ^7Li in ‰ units relative to NIST standard L-SVEC, where $\delta^7Li = [((^7Li/^6Li)_{sample} - (^7Li/^6Li)_{standard})/(^7Li/^6Li)_{standard}] * 1000$. The external precision of the TIMS method was better than ~1.5‰ (2 SD) and ⩽1‰ (2SD) for MC-ICPMS based on repeat measurements of samples and standards. Measurement of δ^7Li in IRMM 016 gave −0.11‰ (±0.77‰, n = 12) and the reproducibility (2 SD) of an in-house granite standard was 0.8‰, n = 7. USGS rock standards G-2 and AGV-1 gave +0.4‰ and +2.6‰ respectively. The basalt standard JB-2 analysed at LSU during this period of study yielded +5.1‰ Chan et al., 2002a. Two samples, the Río los Patos and the ^{7}Li depleted andesite at the southern end of Isla Catal were analyzed by TIMS and MC-ICPMS, and yielded δ^7Li values within the analytical uncertainty.

Strontium isotopes were analyzed using a Micromass Sector 54 instrument at Cornell University following standard cation chromatographic methods. Analyses of NBS 987 during this period yielded 0.710244 ± 0.000006 2σ, n = 40. Oxygen and hydrogen isotopes of water were analyzed by Mountain Mass Spectrometry or at Cornell University using a Finnegan Delta S mass spectrometer equipped with an equilibration device (Godfrey et al., 2003). IAEA and in- house standards were included in each run; precision and accuracy were better than 0.2‰ and 1‰ for δ^{18}O and δD, respectively.

Carbonate mineralogy was determined by powder X-ray diffraction using a Philips 'XPert MRD at Rutgers University. This instrument uses graphite monochromatized Cu Kα radiation (λ = 1.5418 Å) Bragg-Betana data collection mode with a scan range of 4–90° at 0.02°/step and 1 s/step.

3.3. Experimental determination of lithium distribution and isotope fractionation during halite precipitation

In order to constrain the effects of evaporation and halite formation on Li concentrations and isotope composition, an experiment was performed. Twelve mL of a halite-saturated neutral pH solution containing 820 ppm Li was evaporated at room temperature in a PTFE beaker in a HEPA-filtered hood. Over the course of the evaporation experiment ⩽5 μL samples of solution were collected and analyzed for Li and Na concentration and a subset for Li isotopes. At the end of the experiment the halite which formed was washed with methanol to remove any remaining brine and then dissolved in sub-boiling distilled water or ground in methanol to extract brine trapped in inclusions. Samples of ancient lake halite from Hombre Muerto were similarly treated.

4. Results

4.1. Li isotope fractionation during halite formation

Lithium is small relative to the cation site in the halite structure, and partitions into the fluid phase as indicated by the 10-fold increase in the Li/Na ratio of the remaining brine during the halite precipitation experiment (Fig. 2; Table 1). The halite-brine distribution coefficient D, where $D = (Li/Na)_{halite}/(Li/Na)_{brine}$, determined from the Li/Na ratio of the inclusion-free halite and the initial halite-saturated solution, was 0.048. As salt precipitated, the Li/Na ratio of the solution increased, and D decreased to 0.005. The Li in the initial experimental halite saturated brine had a δ^7Li composition of −0.6‰, and after 90% of the water had evaporated it had a composition of +0.4‰, within analytical error of the initial solution. The δ^7Li composition of the brine inclusions was −1.6‰, within error of the initial solution, but slightly more negative and outside the error limit of δ^7Li in the final brine. For Li to substitute for Na in the halite lattice it must change from having 4 water molecules in its inner hydration sphere in fresh water, through a state of 3 water

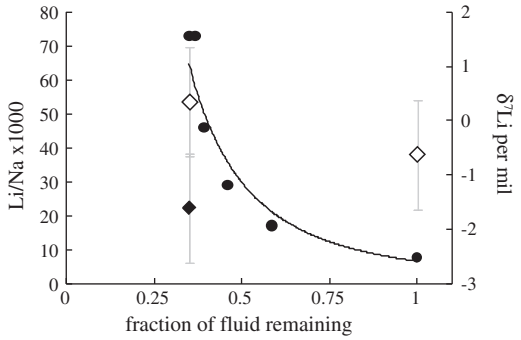

Fig. 2. Results of the experiment to determine the effects of halite formation on the concentration and isotope distribution of Li. Circles Li/Na ratios, diamonds, δ^7Li and open diamond brine, closed diamond brine inclusion (exchanged with halite-bound Li).

molecules and 3 chloride ions in brine (Copestake et al., 1985), to 6 chloride ions in halite. The process could ultimately be associated with an isotopic fractionation factor as high as 1.024 (Yamaji et al., 2001). The lack of isotope fractionation suggests that (1) the step with the largest fractionation factor went to completion or (2) since Li partitions strongly into the brine, brine inclusions may overwhelm the Li inventory of primary lake halite and exchange between lattice-bound and inclusion-bound Li after the halite has formed may shift lattice-bound δ^7Li towards that of the brine. However, if all Li is ultimately incorporated into halite, mass balance requires the initial δ^7Li to be preserved in a sample which is representative of all halite which formed. In summary, the δ^7Li of halite brine inclusions appears to record the δ^7Li of the halite-forming brine.

4.2. Lithium content and isotope composition of Hombre Muerto bedrock and ash weathering experiment

Whole rock Li concentrations and isotope compositions of two Cerro Galán ignimbrites are 25 ppm with +7.0‰, and 106 ppm with +4.9 (Table 2). Quaternary lava flows on Isla Catal have Li concentrations of 18–35 ppm and δ^7Li compositions of −5.2‰ to +1.2‰, while andesite from Cerro Ratones has 20.5 ppm Li and +3.1‰, similar to other arc volcanic rocks (Moriguti and Nakamura, 1998; Chan et al., 2002a; Tomascak et al., 2002). Basement rocks and tourmaline-bearing pegmatites, which are the source of B in the Miocene deposit of Tincalayu (Kasemann et al., 2004), contain 2–65 ppm Li and have δ^7Li between −0.3‰ to +7.2‰ (Table 2). These values are consistent with estimates of the upper continental crust, 0 ± 2‰ and marine metasediments (Teng et al., 2004; Chan et al., 2006). There are no records or accounts of Li-rich pegmatites exposed in the basin, although much of the basement is obscured by the widespread ash deposits of Cerro Galán. A sample of lepidolite and a sample of amblygonite from regional Paleozoic pegmatites have Li concentrations of 2.0% and 8.8%, and a δ^7Li composition of +8.8‰ and +7.6‰, respectively.

Low temperature leaching experiments on the coarse grained 2 Ma old Cerro Galán tuff from Vega Hombre Muerto yielded a leachate which was 5‰ enriched in ^{7}Li relative to the whole rock Li (Table 2). A similar leachate composition resulted from leaching 12 year old ash erupted from Lascar in Chile.

4.3. Geochemical signatures of inflow water to Salar del Hombre Muerto and their relationship to regionally important fluids

The concentration of Li in spring and stream water in the Hombre Muerto drainage basin varies between 0.06 and 6.5 ppm and

Table 1
Li and Sr data for secondary minerals and evaporation experiment.

Sample	Li (ppm)	Li/Na ($\times 10^3$)	δ^7Li	Sr/Na ($\times 10^5$)	$^{87}Sr/^{86}Sr$
Halite precipitation experiment					
Initial brine		8.0	−0.6[b]		
Final brine		73.0	+0.3[b]		
Halite brine inclusion		37.0	+1.6[b]		
Halite matrix		0.37			
Hombre Muerto chemical sediments					
Travertine (aragonite)	42.2		−1.8[a]		0.71534
Halite brine inclusion # 321 (63.8 ka)		0.290	+12.3[b]	7.9	0.71311
Halite matrix #321		0.014			
Halite brine inclusion #351 (86 ka)		0.150	+6.9[b]	4.2	
Halite matrix #351		0.020			

[a] Li isotope analyses at LSU, precision ±1.2 (2s).
[b] Li isotope anaylses at UMD, precision ±1.0 (2s).

Table 2
Li concentration and isotope data for rocks.

Sample	Li (ppm)	δ^7Li
Volcanic rocks		
Ignimbrite at Vega Hombre Muerto (coarse grained)	24.74	+7.0[b]
Washed ash	24.56	+7.2[b]
% Leachable	0.70	+12.6[b]
Ignimbrite near Mina los Patos (fine grained)	106.30	+4.9[b]
Southern Isla Catal andesite	35.20	−5.1[b]; −5.1[c]
Southern Isla Catal basalt	22.60	−3.6[c]
Cerro Ratones andesite	20.45	+3.1[b]
Basement rocks sampled near Mina los Patos		
Garnet biotite schist	21.23	+6.4[c]
Biotite separate	110.00	+2.9[c]
Pegmatite with tourmaline	4.52	−0.3[b]
Augen gneiss	9.52	+0.1[b]
High grade biotite schist with epidote growth	9.65	+7.2[b]
Epidote separate	0.73	
Pegmatite with tourmaline	14.08	+1.1[b]
Pegmatite with tourmaline	3.13	+4.3[b]
Tourmanline separate	31.20	+5.8[c]
Amphibolite	13.51	+1.6[b]
Garnet biotite schist	64.85	+2.3[b]
Biotite separate	118.0	+2.0[c]
Lepidolite (Cachi)	19,532	+8.9[c]
Ambligonite (Cachi)	87,581	+7.6[c]
V. Lascar 1993 erupted ash		
LAS-W bulk	15.8	+2.0[c]
% LAS-W leachable	1.2[a]	+7.6[c]
LAS-S bulk	22.7	+3.1[c]
% LAS-S leachable	0.3[a]	ND

[a] Risacher et al. (2003).
[b] Li isotope analyses at LSU, precision ± 1.2 (2s);
[c] Li isotope anaylses at UMD, precision ± 1.0 (2s).

δ^7Li between +2.5‰ and +7.6‰ (Table 3). The range in concentration and δ^7Li contrast to rivers in other parts of the world where Li concentrations are less than 0.02 ppm (unless they are influenced by geothermal systems or brine) and δ^7Li compositions are between +6‰ and +32‰ because octahedral sites in secondary minerals preferentially incorporate ^{6}Li (Huh et al., 1998, 2001; Bottomley et al., 1999; Chan et al., 2002b; Tomascak et al., 2003; Kisakürek et al., 2005; Pogge van Strandmann et al., 2006, 2010; Vigier et al., 2008, 2010; Millot et al., 2010a; Wimpenny et al., 2010). The springs and streams can be divided between two groups within the basin based on chemical and isotopic compositions (Fig. 3). The composition of the first group is dominated by Na and Cl, have the highest Li/Cl and Li/Na ratios, and δ^7Li values below +4‰. Samples which belong to this group drain Cerro Galán and Cerro Ratones, and include springs around the eastern margin of the salar associated with some of the major basement faults. The other group has variable contributions of HCO_3^- and Ca, and compared to Group 1 has lower Li/Cl and Li/Na and δ^7Li higher than +6‰. It represents springs and streams located around the western side of the salar, which predominantly drain Paleozoic and Cenozoic sedimentary rocks and minor mafic volcanic units of the Incahuasi group. This water chemistry grouping is mostly reflected in their $^{87}Sr/^{86}Sr$ compositions. For example, the Río los Patos and the spring near Mina los Patos have radiogenic Sr compositions of 0.72. This radiogenic character may be derived from the crystalline basement rocks which can have $^{87}Sr/^{86}Sr$ as high as 0.79 (Becchio et al., 1999). While biotite in the Cerro Galán ignimbrite can be sufficiently radiogenic, its Sr concentration is low compared to the whole rock and suggests ignimbrite weathering may be a relatively minor source of Sr because we expect weathering of the glass component should release Sr with a composition similar to the whole rock (Sparks et al., 1985; Kay et al., 2010a,b). In contrast, while the spring at the base of Cerro Ratones is similar to the previous two examples in terms of Na, Cl, and Li, it contains the least radiogenic Sr. Group 2 streams and springs have intermediate $^{87}Sr/^{86}Sr$ (Fig. 3).

Geothermal fluids from the Central Andes occupy the same field as Group 1 on the Durov plot and also have high Li/Na. Geothermal sites located within Miocene and more recent volcanic units have δ^7Li between +2‰ and +4‰, which is also true for Diablo although it is surrounded by crystalline basement rocks. Luracatao and Arizaro have higher δ^7Li for reasons not understood.

4.4. Geochemical signatures of brine

The composition of brine occupying the salar varies spatially although they are all in the Na–Cl–SO_4 family (Table 3). Based on Li and Sr isotope compositions, there are at least two distinct surface brines: brine in the terminal lagoon of the Río los Patos south of Isla Catal (δ^7Li = +7.2; $^{87}Sr/^{86}Sr$ = 0.7197) and brine that emerges at the southern edge of SHM at Vega Trapiche (δ^7Li = +9.4; $^{87}Sr/^{86}Sr$ = 0.7154). While the lagoon forms as a result of inflow of the Río los Patos, its chemical composition evolves not just from evaporative enrichment, but from precipitation of some minerals (notably carbonate and gypsum) and dissolution of others, including halite. Of all the solutes analyzed, Li and SO_4 exhibit the highest enrichment in the lagoon compared to the Río los Patos before it reaches SHM, despite the precipitation of gypsum which removes some sulfate from solution earlier in the evaporation sequence. No change in $^{87}Sr/^{86}Sr$ occurs as the Río los Patos flows to its lagoon indicating there is negligible input of solutes from different sources, but does not rule out incorporation of late stage brine or salts which formed from the river inflow during previous years. The increase in δ^7Li of the lagoon by 2–3‰ relative to the river (Fig. 4) only occurs after evaporation has caused much of the silica to be lost by forming amorphous silicates and Ca by forming carbonate. Since our experiments indicate there is effectively no change in δ^7Li_{brine} when halite forms, either the increase in δ^7Li occurs as gypsum precipitates between Curva los Patos and the lagoon, or as bittern salts precipitate in the final phases of evaporation and remaining brine may leak into the lagoon. This highlights the difference between Sr and Li isotopes, and the necessity to first determine how evaporation might cause δ^7Li to change due to the precipitation of different evaporite minerals before a brine's δ^7Li can be used to infer that of its freshwater parent.

Based on isotopic compositions (δ^7Li = +8.3; $^{87}Sr/^{86}Sr$ = 0.7184), brine in the top 40 m of the halite nucleus is a mixture of different

Table 3
Major and minor element concentrations (ppm) and isotope data of water samples.

Sample	pH	$\delta^{18}O$	δD	SiO_2	Alkanity	Na	K	Mg	Ca	Sr	$^{87}Sr/^{86}Sr$	Cl	Br	SO_4	Li	$\delta^{7}Li$
Rio los Patos (1)	8.74	−5.23	−11.4	79.0	228.75	423	46	13	38	0.82	0.72000	674.8	0.72	58.4	3.33	+2.6[a]; +3.4[b]
Curvalos Patos (2)		5.05	23.39	39.3		1057	120	23	36	1.86	0.71976	1755	1.37	123.6	7.57	+3.9[b]
Lagoon (9)		13.32	60.07			86,980	8535	1720	350	29.22	0.71973	148,720	62.1	17,174	926.2	+7.2[b]
Lagoon Pore fluid (10)		14.06	65.92			84,546	9947	2665	260	25.09	0.71975	150,160	98.1	21,856	1137	+6.6[b]
Rio Trapiche (3)	8.95	−5.83	−46.12	55.1	116.51	30	2	3	30	0.12	0.71322	17.6	0.07	26.4	0.066	+6.6[b]
Vega Hombre Muerto (4)		−6.46	−49.25	80.3		1663	83	23	101	4.24	0.72057	2612	1.32	134.3	5.97	+6.3[b]
Vega Trapiche (11)		12.63	33.9			81,928	8113	3390	1421	66.81	0.71538	157,437	15.8	3450	1615	+9.4[b]
Pore fluid at 2m (13)		5.52	−16.37			91,116	5617	789	695	34.93	0.71950	152,282	28.6	7621	452	+7.9[b]
Well (12)		−7.51	−65.41			92,285	5542	787	538	14.5	0.71843	151,414	10.8	8277	504	+8.3[b]
Chucalaqui (5)	6.9	−9.9	−74.15	48.1	470.31	239	8.4	55.4	66.3	0.16	0.71435	250	0.02	197	0.67	+.6.0[a]
Cerro Ratones Spring	7.05	−7.94	−78.21	98.3	430.05	749	72	43.2	197	3.16	0.71163	1530	0.644	62.5	6.46	+2.5[a]
Mina los Patos (7)	9	−4.67	−55.03	40.6	193.98	293	17.6	21.9	56	0.96	0.72037	330	0.26	214	1.42	+3.1[a]
Incahuasi (8)	8	−9.08	−71.24	61.1	85.4	420	22.4	64.4	118.6	1.58	0.71373	823	0.103	282	3.00	+7.6[a]
Cold spring at dacite dome (14)		−6.47	−48.94		248	32.5	40.2	50.7	182.4	1.82		31.3		29.9	0.28	
(number in parentheses refers to location in Fig. 1)																
Cerro Galan springs																
PUN 1053[c]				99.6		192.5	9.1	9.0	25.3			355.3		21.9	2.6	+4.6[a]
PUN 1054[c]				132.4		313.5	8.1	4.3	19.3			548.2		30.7	5.3	
Galan 1[d]				77.5		1484.6	63.3	0.7	12.0			2166.7		41.5	18.3	+3.3[a]
Galan 2[d]				64.0		60.8	14.8	1.0	6.8			509.0		26.3	0.4	+2.9[a]
Galan 3[d]				77.1		78.0	11.0	3.0	9.0			553.8		22.1	0.8	
Galan 4[d]				66.4		22.0	1.2	1.4	7.8			479.0		12.6	0.1	
Regional geothermal springs																
Antuco				42.7		5358	601.4	239	345			11,231		1357	147.4	+3.0[a]
Diablo 1[e]				8.1		4943	449.4	159	5.0			8558		497.2	33.3	+4.7[a]
Diablo 2[e]				17.3		5237	439.6	164	6.3			9051		522.0	33.3	
Arizaro 1[e]				35.1		62,401	5376	1239	492			159,268		4451	95.3	+18.4[a]
Arizaro 2[e]				33.4		50,859	3535	1040	418			159,253		11,927	99.8	
Aguas Calientes[e]				86.8		5478	368.4	551	843			9385		1970	7.0	
Luracatao[e]				31.6		4179	186.2	83	6.4			5827		186.6	27.7	+10.3[a]
El Tatio 1				134.1		4431	510.3	0.2	245			7706		47.7	39.5	+1.9[a]
El Tatio 2				145.0		4506	507.1	0.1	220			7735		49.5	37.8	
El Tatio 3				161.8		4115	520.5	0.4	224			7961		45.5	37.7	
El Tatio 4				224.6		4934	576.1	0.4	287			8147		34.9	47.5	
El Tatio 5				200.1		3352	152.9	0.2	233			6251		62.4	25.2	
El Tatio 6				195.3		4024	157.6	1.0	256			6084		57.7	28.5	
El Tatio 7				181.8		3279	150.7	0.2	226			5915		63.8	26.2	+1.4[a]
El Tatio 8				139.3		1991	171.8	7.0	87.6			3090		49.9	14.8	

Dilute waters saturated with respect to calcite (C), hydrated Mg–silicates (S); (–) under-saturated all minerals. Calculated, where possible, using PHREEQC (Parkhurst and Appelo, 1999).

[a] Li isotope analyses at UMD, precision ±1.0 (2s).

[b] Li isotope analyses at LSU, precision ±1.2 (2s).

[c] Collected by S. Hynek.

[d] Collected by S. Kay.

[e] Collected by S. Kasemann (locations in Fig. 1, Schmitt et al., 2002).

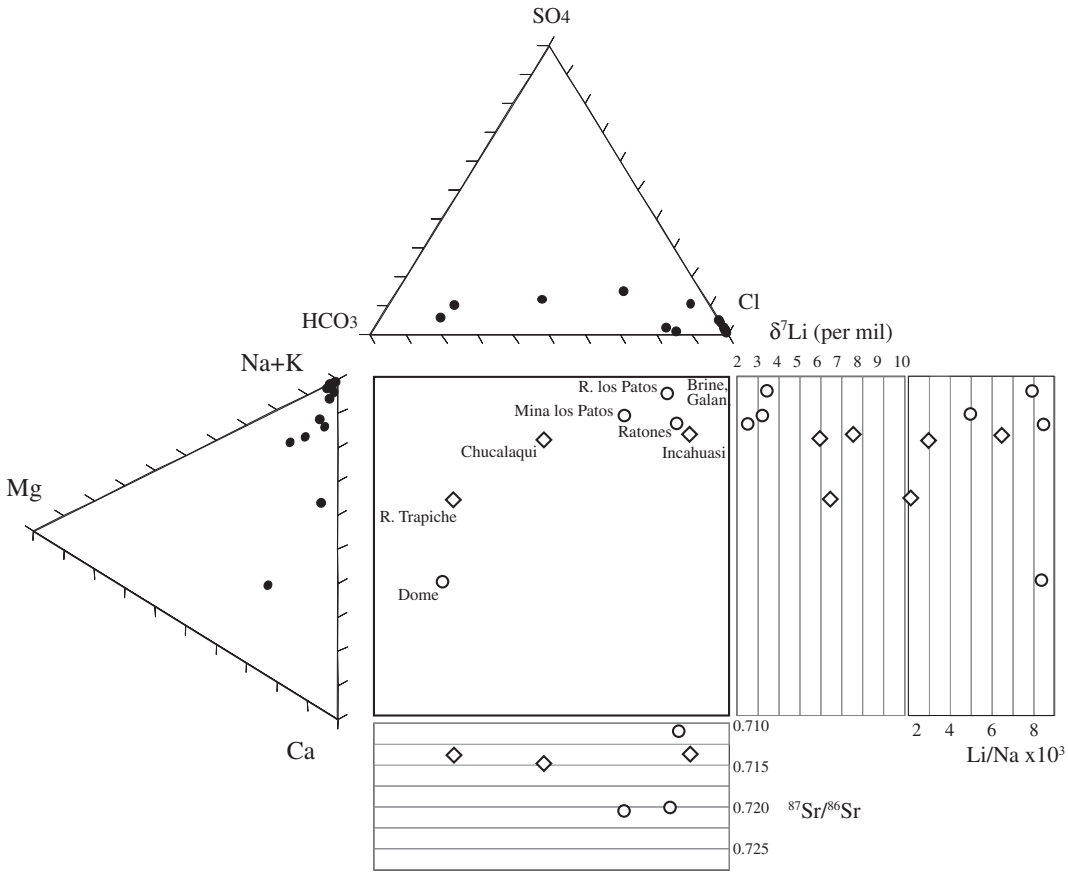

Fig. 3. An extended Durov plot showing the relationships between dilute inflow water Li/Na ratios, higher δ^7Li and ^{87}Sr/^{86}Sr. Circles, fresh water in Group 1, mostly associated with the Río los Patos; diamonds, other freshwater sources in the western part of SHM.

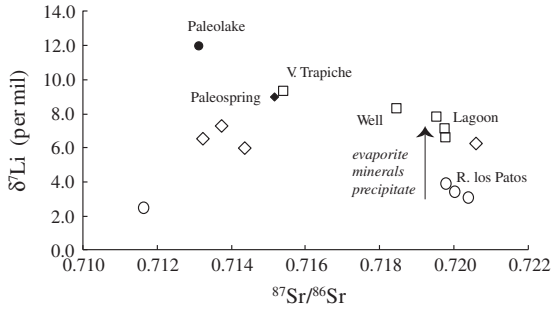

Fig. 4. Relationship between ^{87}Sr/^{86}Sr and δ^7Li. Water in Group 1 which is largely associated with the Río los Patos possess radiogenic Sr and δ^7Li compositions little enriched in ^{7}Li relative to rocks until the formation of evaporite minerals starts to remove ^{6}Li. The precipitation of evaporites has no effect on ^{87}Sr/^{86}Sr so that an evaporating water body will produce a vertical line on this plot. The pumped well plots between the lagoon and Vega Trapiche. The saline water which filled SHM, and captured by halite, plots on an extension of the brine array towards higher δ^7Li. Open symbols as for Fig. 3, closed circle, paleolake halite inclusion, closed diamond paleospring carbonate.

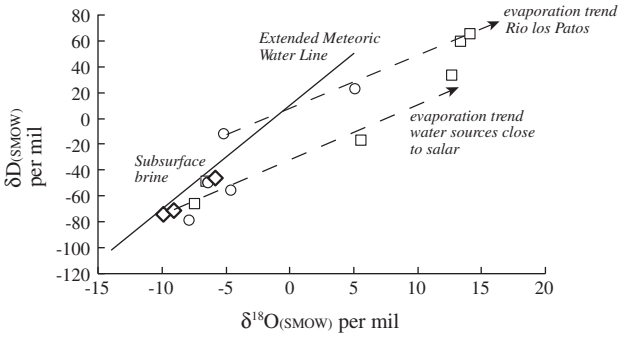

Fig. 5. δ^{18}O–δD for inflow water and brine samples. Symbols as for Fig. 3, δ^{18}O data from Godfrey et al. (2003).

surface brine bodies (Fig. 4). However, the chemical composition of the subsurface brine in the halite nucleus, in particular Li/Cl and Li/Na values which are both lower than in surface brine, suggest it has undergone additional modification. The δ^{18}O and δD compositions of the brine point to the nature of this modification. In arid climates, as water undergoes evaporation its δ^{18}O and δD plot with a shallow slope and fall to the right of, or below, the meteoric water line (MWL). The two SHM surface brines plot well to the right of the MWL indicating they have undergone significant evaporation, but the subsurface brine, during both sampling years, plots close to the MWL (Fig. 5). Since the subsurface brine plots on the MWL, some part of its salt content is acquired by dissolution of soluble evaporite minerals such as halite and bittern salts, and this causes the brine pumped from the well in the halite nucleus to have a lower Li/Na than the surface brine (Fig. 6a). While it is possible that the unevaporated nature of the subsurface brine may reflect increased freshwater inflow towards the center of the salar due to pumping, subsurface brine near the margins of the Salar de Atacama also had δ^{18}O–δD compositions falling on the meteoric water years before that salar was commercially developed (Fritz et al., 1978). Instead we postulate that as the water table lowered with increasing aridity, water entering SHM, except through the lagoon, does so in the subsurface and its evaporation is delayed. This

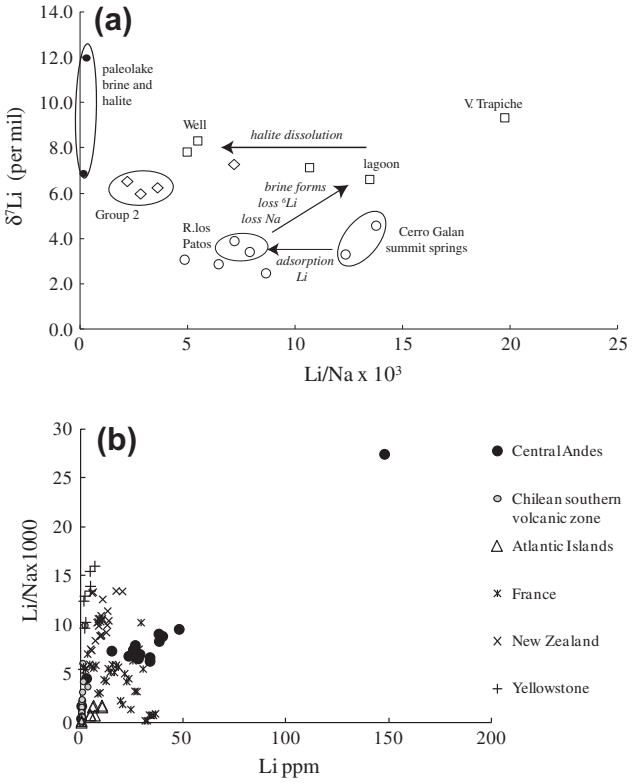

Fig. 6. (a) The adsorption of Li onto the surface of smectite and ferrihydrite as water flows from the volcano summit springs causes negligible fractionation of Li isotopes but decreases Li/Na. The formation of brine by evaporation causes a small increase in δ^7Li, but a large increase in Li/Na due to the precipitation of halite. The subsurface brine contains a component of dissolved halite which has low Li/Na, and draws its position on this plot to the left. If the halite being dissolved was formed in a past saline lake, it will also increase δ^7Li. Symbols as in Fig. 3. (b) The high concentrations of Li in thermal water around the Hombre Muerto drainage basin are shown in context of the Andean southern volcanic zone of Chile plus selected worldwide geothermal locations by the plot of Li/Na ratios versus Li concentrations. Additional data from Giggenbach (1978, 1995), Fournier (1989), Sturchio and Chan (2003), Millot et al. (2007, 2010b, 2012) and Risacher et al. (2011).

does not imply the salar is fossil and losing halite mass, but that dilute, shallow groundwater dissolves salt, and through capillary action rises to the surface where it completely evaporates. This leaves no isotopic imprint on δ^{18}O or δD, but does recycle halite, also indicated by the halite fabric (Lowenstein et al., 2003). Our halite precipitation experiment confirms Li does not partition into the halite structure, and that halite has low Li/Na relative to its parent brine. As a consequence, halite dissolved by shallow groundwater produces brine with lower Li/Na than one formed through evaporation, and one with δ^{18}O that bears no trace of evaporation (Figs. 5 and 6a).

4.5. Li isotope compositions of lake halite and spring carbonate

Two samples of halite formed in perennial lakes early in the last glacial period yielded halite brine inclusion δ^7Li compositions of +7‰ (#351, 86.0 ± 9.3 Ka old) and +12‰ (#321, 63.8 ± 6.8 Ka old) and $(Li/Na)_{halite}$ of 2.0×10^{-5} and 1.4×10^{-5} respectively. δ^7Li of +7‰ is the same as the modern lagoon, but +12‰ is higher than any modern water or brine sample we have analyzed. Using our experimentally determined distribution coefficients, the brine in these ancient lakes had a Li/Na between 0.0003 and 0.004 depending if the brine had just started to form halite or had almost fully evaporated. The lower estimate, which is consistent with the Li/Na of the brine inclusions, is much lower than any of the modern fresh water or brines in the basin today (Fig. 6a). The Sr isotope composition of the brine inclusions, 0.7131, is similar to the streams and springs that drain the western half of the salar (Fig. 4). Since there is no geological evidence for the Río los Patos to have been diverted into a different drainage network, loss of the salars radiogenic signature suggests that this river had a different isotope composition in the past.

Aragonite travertine and geyser structures which formed to the west of Isla Catal about 40 Ka ago (Fleisher, pers. comm.) contain 42 ppm Li with a δ^7Li of −1.8‰. From this a fluid δ^7Li composition of ~+9‰ is predicted, since the δ^7Li of aragonite is 11‰ lower than that of the fluid from which it formed (Marriott et al., 2004). None of the freshwater inflows to the salar have δ^7Li as high as +9‰, although it is comparable to that of some springs in the region, for example Luracatao (Table 3), as well as the subsurface brine and the inferred composition of the pluvial stage lake. The $^{87}Sr/^{86}Sr$ compositions of these travertine deposits are between 0.7148 and 0.7155 (Table 1), similar to minor springs and streams draining the western portion of the salar. In contrast, travertine ridges on the northern margin of the salar flanking the western side of Cerro Ratones were formed from more radiogenic fluids ($^{87}Sr/^{86}Sr$ = 0.7220; Godfrey, unpubl. data), similar to the Río los Patos and to the basement-hosted Mina los Patos spring.

5. Discussion and implications

All streams and springs have low δ^7Li within the Hombre Muerto drainage basin compared to rivers worldwide (Huh et al., 1998), but the δ^7Li of springs and streams which drain the Cerro Galán caldera are particularly low (Table 3). Our leaching experiment on ash of different ages indicates that Li leached by fresh water would be enriched in ^{7}Li relative to the bulk composition of the ash. Leaching experiments in ash erupted from Lascar reported by Risacher and Alonso (2001) showed that the most soluble phase was $CaSO_4$ which they attributed to the incorporation of recycled sedimentary gypsum into the volcanic system of Lascar. The ^{7}Li enrichment of the leachate we measured is consistent with this theory, but incorporation of sedimentary gypsum into Cerro Galán ash is problematic since crystalline basement underlies the volcano (Kay et al., 2010b), not ancient sediments. During the emplacement and cooling of ash flows, we postulate that Li dissolved in associated fluids, condensed volcanic steam or soil water, was trapped in silicate minerals or precipitated with salts such as $CaSO_4$. Secondary minerals such as smectite or illite would have tended to incorporate ^{6}Li leaving ^{7}Li to precipitate with late-forming simple salts which are now readily dissolved, but further investigation would be required to prove this.

Curiously, stream and spring waters in the tuff-covered part of the basin have δ^7Li which are similar to, or lower than, that of the tuffs, not the modestly elevated values obtained from our 51 day long room temperature leaching experiments. River water is, on average, enriched by 18–23‰ in ^{7}Li relative to all rocks except marine chemical sediments (Teng et al., 2004; Chan et al., 2006) because ^{6}Li is lost from solution to secondary minerals in weathering profiles and as it is transported to the oceans (Huh et al., 1998; Pistiner and Henderson, 2003). Since only altered andesites have unusually low δ^7Li, but are volumetrically of minor importance, the similarity of surface water δ^7Li to rocks at Hombre Muerto implies that (1) no secondary minerals are forming, (2) there is a high contribution of Li from thermal springs where high temperatures minimize Li isotope fractionation between liquid and solid phases, or that (3) secondary minerals with low δ^7Li are being leached. The latter seems unlikely because rivers associated with strongly leached horizons are very dilute (Huh et al., 1998, 2001), in contrast to strongly mineralized waters of Hombre Muerto and of the

Central Andes in general. While the kinetics of clay formation are limited by temperature, precipitation (White and Blum, 1995) and biological activity, all of which are low in this high altitude desert (silt and sand comprise the clastic sediments in the Río los Patos delta), the high solute content of the water, especially of silica and Li, is indicative of a geothermal signature, and indeed, most regional geothermal fluids cannot be distinguished from the Río los Patos based on geochemistry (Fouillac and Michard, 1981; Sturchio and Chan 2003; Millot and Négrel, 2007; Millot et al., 2007, 2010b, 2012).

The strongest geothermal signature (high Li/Na and low δ^7Li) is found in springs on the resurgent summit of Cerro Galán (Fig. 6a). Other streams and springs in Group 1 have similar δ^7Li to the springs within the caldera but lower Li/Na, suggesting that any removal of Li has occurred with minimal isotopic fractionation. Considering the suite of secondary minerals likely to occur in the basin and the low surface temperatures, this has occurred through surface adsorption to smectite and ferrihydrite (Pistiner and Henderson, 2003; Vigier et al., 2008, 2010). Streams and springs which drain into the western side of the salar, Group 2, have yet lower Li/Na but higher δ^7Li, suggesting that while their overall high Li content indicates they have a component of geothermal fluid, their δ^7Li has been more affected by loss of ^{6}Li into structural sites of smectite. The difference in Li removal between the two groups may reflect the protolith or the nature of the drainage network, with a tendency for water draining permeable volcaniclastic debris in areas of high topographic relief to not form clays, while the less permeable lithology and low relief around the salar allows clay to form. Alternatively, if there are only a limited number of mineral-sites which can remove Li from solution, only a small proportion of the Li in Li-rich geothermal water on Cerro Galán is removed from solution, and its δ^7Li signature is barely changed. By having a smaller component of geothermal fluid, Group 2's δ^7Li is more strongly affected. One spring of note is Group 1's Mina los Patos which forms a pool bordering a small wetland, an environment in which we expect clays to be abundant. The apparent absence of any increase in δ^7Li suggests a low, possibly negative δ^7Li initial composition of inflow water or that too little Li is removed by clays for it to affect δ^7Li of the water. This spring is located on one of the largest regional faults which transect the basin, and the similarity of the Li data to others of Group 1 suggests that flow through this fault is sufficiently high that its δ^7Li does not evolve any more than other Group 1 fluids.

According to the composition of halite inclusions, the paleolake that covered the salar during wet climate states had much lower Li/Na and higher δ^7Li higher than any modern water or brine (Fig. 6a). These chemical and isotopic properties may be similar to groundwater that infiltrated during pluvial climates. Similarly low Li/Na ratios have been measured in river water draining arc tephras, but in a wet climate (Dessert et al., 2009). The low Li/Na of the ancient lake suggests that with an increased hydrologic budget, either more Li was sequestered by clays or hydrothermal fluids were more diluted by meteoric water. Either of these scenarios is consistent with a higher δ^7Li by incorporation of ^{6}Li in clays or by making the δ^7Li of run-off more similar to the experiments of ash leaching. Since the paleolake's Sr isotope composition also changed relative to the modern lagoon (0.71311 versus 0.71973; Fig. 4), becoming more similar to the whole rock composition of the Cerro Galán tuffs, dilution of hydrothermal water during past pluvial climates by low temperature weathering of the ignimbrites appears to have been of greater importance. It has been noted that the activity of other spring systems in the Puna have also changed as climate conditions fluctuated between arid and more humid conditions relative to a constant heat flux (Gibert et al., 2009). However the analysis of lake halite in this study indicates that the activity or dilution of hot spring water may influence the chemical composition of surface and shallow groundwater on basin-wide scales in this volcanically active area.

Because our survey did not find any rocks particularly enriched in Li within the drainage basin, we conclude that the Li resource represents the accumulation of Li sourced from geothermal fluids and rock weathering with minor clay formation. One important implication of the change in climate is that accumulation of the Li resource has been episodic. If a flow of 1.6 m^3/s for the Río los Patos (based on measurements during 1992; data from Hombre Muerto EIS, Water Management Consultants, 1992) and a Na concentration of 420 ppm are representative of modern conditions, it would take 450 Ka to form the amount of halite above a lake-bed halite directly dated at 85 Ka and now at a depth of 40.7 m in the 300 km^2 halite nucleus (Godfrey et al., 2003). The conflict between the 85 Ka age of the salt formation and the current influx of Na suggests that an additional source of salt is not accounted for by surface inflow, such as the recycling of salt from older halite units. In contrast, the 3 ppm dissolved Li concentration of the Río los Patos implies it would take a much shorter time, less than 5 Ka, to accumulate the 0.8×10^9 kg Li deposit now found in the top 40 m of the halite nucleus showing that the weathering flux of Li and Na can decouple according to climate state.

The Central Andes is a volcanic region with many closed drainage basins containing Li-rich brine. Salt lakes and pans occupying closed basins surrounded by volcanic rocks are found in other regions of the world, but few have Li concentrations comparable to those of the Central Andes (Evans, 2008). The surface geology of the Central Andes is dominated by volcanic rocks, especially ash which contains readily soluble glass; there are also many hydrothermal springs which are active, or have recently been so. Geothermal fluids from other locations worldwide, including the southern Andes of Chile, have as high or higher Li/Na ratios (Giggenbach, 1978, 1995; Gougel, 1983; Fournier, 1989; Sturchio and Chan, 2003; Cortecci et al., 2005; Millot and Négrel, 2007; Millot et al., 2007, 2010b, 2012; Risacher et al., 2011), but compared to those from the Central Andes their Li concentrations tend to be lower (Fig. 6b). It is possible that more Li can be lost from spring water in temperate areas because there is more clay formation between the hydrothermal cell where Li is dissolved and the point where the springs emanate, or that thermal springs in the Central Andes entrain additional sources of Li. Risacher et al. (2011) suggested that many thermal springs in Northern Chile contain some fraction of brine leaked from salars, a model which should be applicable to arid Northwest Argentina. If surface brine had been entrained by thermal springs, we would expect it to have relatively high δ^7Li. It is possible that a spring at Salar de Arizaro whose water has low Li/Na and high δ^7Li (Table 3) does have sedimentary brine mixed with a thermal fluid. Nevertheless, that example is anomalous within the small set of springs we have analyzed, although it is clear that the influence of recycled brines cannot be overlooked.

6. Summary

An experiment to determine the isotopic fractionation of Li during the formation of halite indicates that any fractionation which might occur cannot be resolved by current measurement techniques, and that primary halite is a material which can preserve the Li isotopic composition of ancient brine. The evaporation of fresh water to concentrations where halite precipitates may cause a small increase in δ^7Li as minerals form earlier in the evaporation sequence, but further work is required to determine which minerals are responsible. Unlike ^{87}Sr/^{86}Sr, which is a conservative property during brine formation, measurement of fresh water δ^7Li should not be assumed to be identical to the δ^7Li of a brine or halite

that may form by evaporation and vice versa. However, with these constraints, it has been possible to address the isotope budget of Li in Salar del Hombre Muerto's drainage basin and brine.

Hombre Muerto salar is the terminal point of a drainage basin which includes a large part of the Cerro Galán caldera. Geothermal activity and weathering of the volcanic deposits produces water rich in Li relative to Na, and with a Li isotope composition similar to the protolith, which indicates there is little Li isotopic fractionation due to the formation of secondary minerals in this high altitude desert. Water sources in areas closer to SHM with lower relief, and where bedrock lithology includes sedimentary rocks, are also enriched in Li relative to rivers on a global scale, but have had their Li/Na and isotope compositions modified by clay formation compared to the high relief volcanic part of the basin. Spring carbonates and brine-inclusions in the salt which fills SHM indicate that water which formed a salt lake during pluvial climates in the past had a different composition, with lower Li/Na, higher δ^7Li, and less radiogenic Sr. While the slower accumulation of the Li resource and lower Li/Na under a wet climate can reflect increased precipitation diluting a geothermal Li input, we propose that it was also accompanied by an increase in clay formation which sequestered Li, and in particular ^{6}Li.

Today's conditions of dry climate and geothermal activity are common to many other basins in the Central Andes, and other tectonically active desert-belt regions. Decoupling the flux of Li in run-off from other major cations such as Na occurred when the ratio of geothermal to cold surface water changed with climate. This caused episodic accumulation of the Li resource at Salar del Hombre Muerto, and may characterize other Li-brine resources in the Central Andes.

Acknowledgements

We would like to thank Minera del Altiplano (FMC), especially Daniel Chavez Diaz, Gonzalo Tufiño and Rodolfo Mendoza for access to samples and logistical assistance. We would also like to thank Raúl Gutierrez of Borax Argentina SA for his assistance with the collection of water samples. Simone Kasemann, Sue Kay and Scott Hynek provided samples of thermal spring water; and Randall Marrett aided with field studies. The manuscript benefited from all the reviews. This work was supported by NSF Grants ATM-9631291and ATM-9709771 to T.E.J., and ATM-9632359 to T.K.L. Lithium isotope work was supported by National Science Foundation Grants EAR-9506390 and OCE-9905540 to L.H. Chan, EAR 0948549 to W.F.M., and by the ICR policy of the Rutgers School of Environmental and Biological Sciences.

References

Becchio, R., Lucassen, F., Kasemann, S., Franz, G., Viramonte, J., 1999. Geoquímica y sistemática isotópica de rocas metamórficas del Paleozoico inferior. Noreste de Argentina y Norte de Chile (21°–27°S). Acta Geol. Hispan. 34, 273–299.

Bobst, A.L., Lowenstein, T.K., Jordan, T.E., Godfrey, L.V., Ku, T.-L., Luo, S., 2001. A 106 ka paleoclimate record from drill core of the Salar de Atacama, northern Chile. Palaeogeogr. Palaeoclim. Palaeoecol. 173, 21–42.

Bottomley, D.J., Katz, A., Chan, L.-H., Starinsky, A., Douglas, M., Clark, I.D., Raven, K.G., 1999. The origin and evolution of Canadian Shield brines: evaporation or freezing of seawater? New lithium isotope and geochemical evidence from the Slave craton. Chem. Geol. 155, 295–320.

Chan, L.-H., Leeman, W.P., You, C.-F., 2002a. Lithium isotope composition of Central American volcanic arc lavas: implications for modification of subarc mantle by slab-derived fluids: correction. Chem. Geol. 182, 293–300.

Chan, L.-H., Starinsky, A., Katz, A., 2002b. The behavior of lithium and its isotopes in oilfield brines: evidence from the Heletz–Kokhav field, Israel. Geochim. Cosmochim. Acta 66, 615–623.

Chan, L.-H., Leeman, W.P., Planks, T., 2006. Lithium isotopic composition of marine sediments. Geochem. Geophys. Geosyst. Q06005. http://dx.doi.org/10.1029/2005GC001202.

Copestake, A.P., Neilsen, G.W., Enderby, J.E., 1985. The structure of a highly concentrated aqueous solution of lithium chloride. J. Phys. Chem.: Solid State Phys. 18, 4211–4216.

Cortecci, G., Boschetti, T., Mussi, M., Herrera Lameli, C., Mucchino, C., Barbieri, M., 2005. New chenmical and original isotopic data on waters from El Tatio geothermal field, northern Chile. Geochem. J. 39, 547–571.

Dessert, C., Gaillardet, J., Dupre, B., Schott, J., Pokrovsky, O.S., 2009. Fluxes of high- versus low-temperature water–rock interactions in aerial volcanic areas: example from the Kamchatka Peninsula, Russia, 2009. Geochim. Cosmochim. Acta 73, 148–169.

Evans, K., 2008. Know limits: an abundance of lithium. Ind. Miner. 63, 48–55.

Fouillac, C., Michard, G., 1981. Sodium/lithium ratio in water applied to geothermometry of geothermal reservoirs. Geothermics 10, 55–70.

Fournier, R.O., 1989. Geochemistry and dynamics of the Yellowstone National Park hydrothermal system. Ann. Rev. Earth Planet. Sci. 17, 13–53.

Fritz, S.C., Baker, P.A., Lowenstein, T.K., Seltzer, G.O., Rigsbly, C.A., Dwyer, G.S., Tapia, P.M., Arnold, K.K., Ku, T.-L., Luo, S., 2004. Hydrologic variation during the last 170,000 years in the southern hemisphere tropics of South America. Quatern. Res. 61, 95–104.

Fritz, P., Silva, C., Suzuki, O., Salati, E., 1978. Isotope hydrology in Northern Chile. In: Proceedings of the Symposium Isotope Hydrology. IAEA, Vienna, pp. 525–543.

Gibert, R.O., Taberner, C., Sáez, A., Giralt, S., Alonso, R.A., Edwards, R.L., Pueyo, J.J., 2009. Igneous origin of CO_2 in ancient and recent hot-spring waters and travertines from the northern Argentinean Andes. J. Sediment. Res. 79, 554–567.

Giggenbach, W.F., 1978. The isotopic composition of waters from the El Tatio geothermal field, Northern Chile. Geochim. Cosmochim. Acta 42, 979–988.

Giggenbach, W.F., 1995. Variations in the chemical and isotopic compositions of fluids discharged from the Taupo Volcanic Zone, New Zealand. J. Volcanol. Geotherm. Res. 68, 89–116.

Godfrey, L.V., Jordan, T.E., Lowenstein, Alonso, R., 2003. Stable isotope constraints on the transport of water to the Andes between 22° and 26°S during the last glacial cycle. Palaeogeogr. Palaeoclim. Palaeoecol. 194, 299–317.

Gougel, R., 1983. The rare alkalis in hydrothemal alteration at Wairakei and Braodlands, geothermal fields. N.Z. Geochim. Cosmochim. Acta 47, 429–437.

Heit, B., Yuan, X., Kind, R., Kay, S., Sandvol, E., Alonso, R., Coira, B., Comte, D., 2010. Receiver function results from the PUDEL (Puna DELamination) seismic array in the Southern Puna plateau. Geophys. Res. Abstr., 12, EUG2010-14192.

Houston, J., Butcher, A., Ehren, P., Evans, K., Godfrey, L., 2011. The evaluation of brine prospects and the requirement for modifications to filing standards. Econ. Geol. 106, 1225–1239.

Huh, Y., Chan, L.-H., Zhang, L., Edmond, J.M., 1998. Lithium and its isotopes in major rivers: implications for weathering and the oceanic budget. Geochim. Cosmochim. Acta 62, 2039–2051.

Huh, Y., Chan, L.-H., Edmond, J.M., 2001. Lithium isotopes as a probe of weathering processes: Orinoco River. Earth Planet. Sci. Lett. 194, 189–199.

Ide, Y.F., Kunasz, I.A., 1989. Origin of lithium in Salar de Atacama, northern Chile. In: Erickson, G.E., Cānas Pinochet, M.T., Reinemund, J.A. (Eds.), Geology of the Andes and Its Relation to Hydrocarbon and Mineral Resources, vol. 11. Circum-Pacific Council for Energy and Mineral Resources, Earth Science Series, Houston, Texas, pp. 165–172.

Jeffcoate, A.B., Elliott, T., Thomas, A., Bouman, C., 2004. Precise, small sample size determinations of lithium isotopic compositions of geological reference materials and modern seawater by MC-ICP-MS. Geostandards Geoanal. Res. 28, 161–172.

Jordan, T.E., Alonso, R.N., Godfrey, L.V., 1999. Tectónica, subsidencia y aguas en el Salar del Hombre Muerto, Puna, Argentina: XIV Congresso Geologica Argentino, vol. 1, pp. 254–256.

Kasemann, S.A., Meixner, A., Viramonte, J.G., Alonso, R.N., Franz, G., 2004. Boron isotope composition of geothermal fluids and borate minerals from salar deposits (central Andes/NW Argentina). J. S. Am. Earth Sci. 16, 685–697.

Kay, S.M., Coira, B., Wörner, G., Kay, R.W., Singer, B.S., 2010a. Geochemical, isotopic and single crystal ^{40}Ar/^{39}Ar age constraints on the evolution of the Cerro Galán ignimbrites. Bull. Volcanol.. http://dx.doi.org/10.1007/s00445-010-0410-7.

Kay, S.M., Coira, B., Caffe, P.J., Chen, C.-H., 2010b. Regional chemical diversity, crustal and mantle sources and evolution of central Andean Puna plateau ignimbrites. J. Volcanol. Geotherm. Res. 198, 81–111.

Kisakürek, B., James, R.H., Harris, N.B.W., 2005. Li and δ^7Li in Himalayan rivers: proxies for silicate weathering? Earth Planet. Sci. Lett. 237, 387–401.

Linares, E., González, R., 1990. Catálogo de edades radiométricas de la República Argentina: 1957–1987. Asociación Geológica Argentina Serie B, Buenos Aires. 19, 628 p.

Lowenstein, T.K., Li, J., Godfrey, L.V., Jordan, T.E., 1996. Andean Climate History from a Holocene–Pleistocene Salt Core, Salar del Hombre Muerto, Argentina. GSA Abstr.

Lowenstein, T.K., Hein, M.C., Bobst, A.L., Jordan, T.E., Ku, T.-L., Luo, S., 2003. An assessment of stratigraphic completeness in climate-sensitive closed-basin lake sediments: Salar de Atacama, Chile. J. Sediment. Res. 73, 91–104.

Marriott, C.S., Henderson, G.M., Crompton, R., Staubwasser, M., Shaw, S., 2004. Effect of mineralogy, salinity, and temperature on Li/Ca and Li isotope composition of calcium carbonate. Chem. Geol. 212, 5–15.

Millot, R., Négrel, P., 2007. Multi-isotopic tracing (δ^7Li, δ^{11}B, ^{87}Sr/^{86}Sr) and chemical geothermometry: evidence from hydro-geothermal systems in France. Chem. Geol. 244, 664–678.

Millot, R., Négrel, P., Petelet-Giraud, E., 2007. Multi-isotopic (Li, B, Sr, Nd) approach for geothermal reservoir characterization in the Limagne Basin (Massif central, France). Appl. Geochem. 22, 2307–2325.

Millot, R., Vigier, N., Gaillardet, J., 2010a. Behaviour of lithium and its isotopes during weathering in the Mackenzie Basin, Canada. Geochim. Cosmochim. Acta 74, 3897–3912.

Millot, R., Scaillet, B., Sanjuan, B., 2010b. Lithium isotopes in island arc geothermal systems: Guadeloupe, Martinique (French West Indies) and experimental approach. Geochim. Cosmochim. Acta 74, 1852–1871.
Millot, R., Hegan, A., Négrel, O., 2012. Geothermal waters from the Taupo Volcanic Zone, New Zealand: Li, B and Sr isotopes characterization. Appl. Geochem. 27, 677–688.
Moriguti, T., Nakamura, E., 1998. Across-arc variation of Li isotopes in lavas and implications for crust/mantle recycling at subduction zones. Earth Planet. Sci. Lett. 163, 167–174.
Parkhurst, D.L., Appelo, C.A.J., 1999. User's Guide to PHREEQC (Version 2)—A Computer Program for Speciation, Batch-Reaction, One-Dimensional Transport, and Inverse Geochemical Calculations. U.S. Geol. Survey Water-Res. Investigations Report 99-4259, 310 p.
Pistiner, J.S., Henderson, G.M., 2003. Lithium-isotope fractionation during continental weathering processes. Earth Planet. Sci. Lett. 6738, 1–13.
Placzek, C., Quade, J., Patchett, P.J., 2006. Geochronology and stratigraphy of late Pleistocene lake cycles on the southern Bolivian Altiplano: implications for causes of tropical climate change. Bull. Geol. Soc. Am. 118, 515–523.
Pogge van Strandmann, P.A.E., Burton, K.W., James, R.H., van Calsteren, P., Gislason, S.R., Mokadem, F., 2006. Riverine behaviour of uranium and lithium isotopes in an actively glaciated basaltic terrain. Earth Planet. Sci. Lett. 251, 134–147.
Pogge van Strandmann, P.A.E., Burton, K.W., James, R.H., van Calsteren, P., Gislason, S.R., 2010. Assessing the role of climate on uranium and lithium isotope behaviour in rivers draining a basaltic terrain. Chem. Geol. 270, 227–239.
Risacher, F., Alonso, H., 2001. Geochemistry of ash leachates from the 1993 Lascar eruption, northern Chile. Implication for recycling of ancient evaporites. J Volcanol. Geotherm. Res. 109, 319–337.
Risacher, F., Alonso, H., Salazar, C., 2003. The origin of brines and salts in Chilean salars: a hydrochemical review. Earth-Sci. Rev. 1293, 1–45.
Risacher, F., Fritz, B., Hauser, A., 2011. Origin of components in Chilean thermal waters. J. S. Am. Earth Sci. 31, 153–170.
Risse, A., Trumbull, R.B., Coira, B., Kay, S.M., van den Bogaard, P., 2008. $^{40}Ar/^{39}Ar$ geochronology of mafic volcanism in the back-arc region of the southern Puna plateau, Argentina. J. S. Am. Earth Sci. 26, 1–15.
Rosko, M., Jaacks, J., 2012. Measured, Indicated and Inferred Lithium and Potassium Resource, Sal de Vida Project Salar del Hombre Muerto, Catamarca-Salta, Argentina. Report for NI 43-101 Prepared on Behalf of Lithium One Inc., 332 p.
Schmitt, A.K., Kasemann, S., Meixner, A., Rhede, D., 2002. Boron in central Andean ignimbrites: implications for crustal boron cycles in an active continental margin. Chem. Geol. 183, 333–347.
Sparks, R.S.J., Francis, P.W., Hamer, R.D., Pankhurst, R.J., O'Callaghan, L.O., Thorpe, R.S., Pahe, R., 1985. Ignimbrites of the Cerro Galan caldera NW Argentina. J. Volcanol. Geotherm. Res. 24, 205–248.
Sturchio, N.C., Chan, L.-H., 2003. Lithium isotope geochemistry of the Yellowstone hydrothermal system. Soc. Econ. Geol. Spec. Publ. 10, 171–180.
Teng, F.-Z., McDonough, W.F., Rudnick, R.L., Dalpe, C., Tomascak, P.B., Chappell, B.W., Gao, S., 2004. Lithium isotopic composition and concentration of the upper continental crust. Geochim. Cosmochim. Acta 68, 4167–4178.
Tomascak, P.B., Carlson, R.W., Shirey, S.B., 1999. Accurate and precise determination of Li isotopic compositions by multi-collector sector ICP-MS. Chem. Geol. 158, 145–154.
Tomascak, P.B., Widom, E., Benton, L.D., Goldstein, S.L., Ryan, J.G., 2002. The control of lithium budgets in island arcs. Earth Planet. Sci. Lett. 196, 227–238.
Tomascak, P.B., Hemming, N.G., Hemming, S.R., 2003. The lithium isotopic composition of waters of the Mono Basin, California. Geochim. Cosmochim. Acta 67, 601–611.
Vigier, N., Decarreau, A., Millot, R., Carignan, J., Petit, S., France-Lanord, C., 2008. Quantifying Li isotope fractionation during smectite formation and implications for the Li-cycle. Geochim. Cosmchim. Acta 72, 780–792.
Vigier, N., Decarreau, A., Millot, R., Petit, S., 2010. Quantifying lithium isotope fractionation during clay formation at low temperatures. Geophys. Res. Abstr., 12, EGU2010-11160.
Wimpenny, J., James, R.H., Burton, K.W., Gannoun, A., Mokadem, F., Gíslason, S.R., 2010. Glacial effects on weathering processes: new insights from the elemental and lithium isotopic composition of West Greenland rivers. Earth Planet. Sci. Lett. 290, 427–437.
White, A.F., Blum, A.E., 1995. Effects of climate on chemical weathering in watersheds. Geochim. Cosmochim. Acta 59, 1729–1747.
Yamaji, K., Makita, Y., Watanabe, H., Sonoda, A., Kanoh, H., Hirotsu, T., Ooi, K., 2001. Theoretical estimation of lithium isotopic reduced partition function for lithium ions in aqueous solution. J. Phys. Chem. A 105, 602–613.
You, C.F., Chan, L.-H., 1996. Precise determination of lithium isotopic composition in low concentration natural samples. Geochim. Cosmochim. Acta 60, 909–915.